

Synthesis of Propylene Glycol Monomethyl Ether Over Mg/Al Hydrotalcite Catalyst

Hong-yan Zeng · Ya-ju Wang · Zhen Feng ·
Kui-yi You · Ce Zhao · Jin-wei Sun · Ping-le Liu

Received: 18 November 2009 / Accepted: 29 March 2010 / Published online: 10 April 2010
© Springer Science+Business Media, LLC 2010

Abstract Mg–Al hydrotalcites with different Mg/Al molar ratios were prepared and characterized by XRD, FT-IR, SEM and BET analyses. The calcined hydrotalcite with Mg/Al molar ratio of 4.0 (LDO Mg/Al 4.0) exhibited the highest catalytic activity in the synthesis of propylene glycol methyl ether (PM). The catalytic activity relating to the amount of the basic sites and crystallinity depended on the Mg/Al molar ratio. The optimal equilibrium of acid–base property and high crystallinity made the LDO Mg/Al 4.0 an excellent catalyst in the reaction. Etherification of propylene oxide (PO) with methanol over the LDO Mg/Al 4.0 was researched. The optimized reaction conditions were as follows: 140 °C, catalyst amount 0.9 wt%, methanol/PO molar ratio 4.0 and 6 h. The PO conversion and PM selectivity were 93.2 and 97.4%, respectively. Above all, almost all the PM was 1-methoxy-2-propanol, for no 2-methoxy-1-propanol was detected by GC analysis in the reaction products, and the catalyst could be reused for five times.

Keywords Mg–Al hydrotalcite · Propylene oxide · Propylene glycol monomethyl ether · Catalyst

1 Introduction

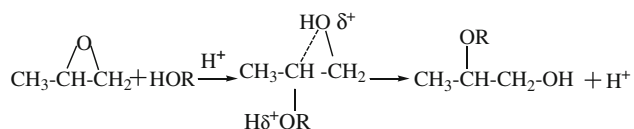
Glycol ether is a component of many commercial products, such as air freshener, antifreeze, cosmetic product and plastics [1]. Because of the low toxicity of propylene

glycol ether, it is expected as a safe substitute for toxic ethylene glycol ether [2]. Propylene glycol monomethyl ether (PM) is a member of the family of glycol ether with a wide variety of consumer products and industrial applications. PM is used in the chemical, agricultural, automotive, paint, lacquer, and varnish industry [3]. Its predominant use is as a solvent in various manufacturing processes and as a chemical building block for the manufacture of propylene glycol methyl ether acetate. PM is produced commercially by reacting propylene oxide (PO) with methanol in the presence of catalyst. Due to the asymmetry of propylene oxide, the epoxide ring of propylene oxide may open either at the C–O bonds, so that the reaction yields a mixture of two isomers with the α -isomer, 1-methoxy-2-propanol (PPM) and the β -isomer, 2-methoxy-1-propanol. Among the products, PPM has a lower toxicity than 2-methoxy-1-propanol, so high selectivity is required for the reaction [2]. Acid catalysts, such as BF_3 , heteropolyacids and solid acids, can be used for the reaction and appear to exhibit good catalytic activity, but they inevitably produce undesirable 2-methoxy-1-propanol and other byproducts. The epoxy ring of PO may preferentially open at the least sterically hindered position over the basic catalyst and lead to most secondary alcohol PPM [2, 4–6]. Homogenous base catalysts such as sodium methoxide and NaOH, show high activity and selectivity, but they suffer from the drawbacks of separation, liquid waste treatment and corrosion [4, 7]. The replacement of currently used homogeneous alkaline catalysts by solid catalysts can result in catalyst reuse and waste stream reduction and make the process of industrial production environmentally benign and economical because of their non-corrosiveness and easy separation from products [8]. Zhang et al. [4] reported that MgO which showed PO conversion 71.0% and PPM selectivity 92.0% was found to be more active and selective than CaO

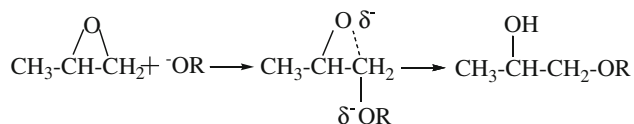
H. Zeng (✉) · Y. Wang · Z. Feng · K. You · C. Zhao ·
J. Sun · P. Liu
College of Chemical Engineering, Xiangtan University,
Xiangtan 411105, Hunan, China
e-mail: hongyanzeng99@hotmail.com; hyzeng@xtu.edu.cn

for the formation of 1-methoxy-2-propanol. Al₂O₃ showed high PO conversion 98.2%, but low PPM selectivity 75.0%.

Acid-catalyzed reaction



Basic-catalyzed reaction



In recent years, some patents and papers have shown that synthetic anionic double hydroxide clays are efficient and selective catalysts for the synthesis of glycol ether [2, 9, 10]. However, the hydrotalcites have not been studied sufficiently so far. Only a few papers covering the influence of acid-base properties of layered double oxides on the synthesis of PM have been published, and in the literatures, the PPM selectivity are low [2, 7]. Recently, it was found that Mg–Al hydrotalcites showed the high activity and selectivity to the desired product PPM in the synthesis of PM. In this study, a series of Mg–Al hydrotalcites with various Mg/Al molar ratios were studied for improving the activity and selectivity of the Mg–Al hydrotalcite catalyst. The characterization of the Mg–Al hydrotalcites was studied with XRD, FT-IR, SEM, BET and Hammett titration method and the relationship between structure and catalytic performance was discussed, which might give fundamental insight into the catalytic mechanism of the catalyst.

2 Experimental

2.1 Catalyst Preparation

All the Mg–Al hydrotalcites were prepared by urea method (urea/NO₃[−] molar ratio of 4.0) [11]. An aqueous solution containing various Mg/Al molar ratios of Mg(NO₃)₂·6H₂O and Al(NO₃)₃·9H₂O was placed into a three-neck flask. The solution was maintained at 105 °C for 12 h under stirring (300 rpm), and then aged statically at the same temperature for another 18 h. The formed solids were collected by filtration and washed with deionized water, and subsequently dried at 100 °C for 18 h, which were denoted as LDHs. Part of the LDHs were calcined at

500 °C for 7 h in a muffle furnace, which were designated as LDOs.

2.2 Catalyst Characterization

Powder X-ray diffraction (XRD) patterns were obtained in the 2θ range 3–70° using a Rigaku D/MAX-3C instrument with Cu Kα source (λ = 0.1541 nm), and the X-ray patterns were indexed according to the JCPDS database. FT-IR spectrum was recorded on Perkin-Elmer Spectrum One B instrument using KBr pellet technique. Scanning electron micrograph (SEM) was obtained with a JEOL JSM-6700F instrument. The specific surface areas were calculated using the Brunauer–Emmett–Teller (BET) method based on the N₂ adsorption isotherms. To measure the basic strengths of the Mg–Al hydrotalcites, the following Hammett indicators were used: bromothymol blue (H_− = 7.2), phenolphthalein (H_− = 9.8), 2,4-dinitroaniline (H_− = 15.0) and nitroaniline (H_− = 18.4). About 0.05 g of samples were shaken with a methanol solution of Hammett indicators (5 mL) and left to equilibrate for 2 h after which no further color changes were observed. The basic strength is quoted as being stronger than the weakest indicator which exhibits a color change, but weaker than the strongest indicator that produces no change. To measure the basicity of the Mg–Al hydrotalcites, the method of Hammett indicator-benzene carboxylic acid titration was used [12].

2.3 Catalyst Test

The reactions were carried out in a sealed stainless-steel autoclave (500 mL), equipped with mechanical stirring and sampling device. In the reactor, an amount of methanol, propylene oxide and the catalyst were poured before closing. After purging for 10 min with N₂ flow, the mixture was heated to the reaction temperature. When the reaction was over, the mixture was cooled down to room temperature. The solid catalyst was filtered, washed with methanol, then dried, and used for the recycling test. The reaction products were analyzed on a gas chromatograph (Agilent 6980N with a flame ionization detector) equipped with a 30-m DB-1 capillary column. The carrier gas N₂ (19.0 mL min^{−1}) and the oven temperature program consisted of: start at 40 °C, ramp at 10 °C min^{−1} to 200 °C (16 min) with injector and detector temperature 250 °C. The *n*-hexane was used as the internal standard.

2.4 Orthogonal Method

A 4-factor plus 4-level L₁₆ (4⁴) orthogonal experimental design was applied to determine the optimal conditions [13]. The orthogonal experimental design was an effective

Table 1 Factors and levels of the $L_{16}(4^4)$ orthogonal experiments

Level	Factor			
	Temperature (°C) T	Methanol/PO molar ratio M	Catalyst amount (wt%) A	Time (h) t
1	80	4:1	0.6	2
2	100	3:1	0.9	4
3	120	2:1	1.2	6
4	140	1:1	1.5	8

method for investigating the effect of the factors on the PO conversion and PM selectivity by reducing the experimental numbers. Furthermore, the optimal reaction conditions and the significance of every factor's effect on the PO conversion and PM selectivity could be obtained. Four independent experimental variables, namely reaction temperature (T), methanol/PO molar ratio (M), catalyst amount (wt% of total reactants, A) and reaction time (t) were selected as controlled factors. The data were analyzed by analysis of variance (ANOVA). The factors and levels in the orthogonal experiment were given in Table 1. The PO conversion and PM selectivity were defined as the following equations, respectively.

$$\text{PO conversion} = \frac{m_{\text{POactual}}}{m_{\text{POtheoretical}}} \times 100\%$$

$$\text{PM selectivity} = \frac{m_{\text{PM}}}{m} \times 100\%$$

where the m_{POactual} (g) and $m_{\text{POtheoretical}}$ (g) were the mass of PO reacted actually and theoretically, respectively. The m_{PM} and m were the mass of PM obtained actually and PM produced by m_{POactual} theoretically, respectively.

2.5 Statistical Analysis

All the experiments were carried out three times in order to determine the variability of the results and to assess the experimental errors. In this way, the arithmetical averages and the standard deviations were calculated for all the results.

3 Results and Discussion

3.1 Microstructural Studies

3.1.1 XRD Analysis

Figure 1 demonstrated the XRD patterns of the Mg/Al hydrotalcites with different Mg/Al molar ratios. Indexing of the diffraction peaks was done using standard JCPDS file 22-700 [14]. Clearly, the structural properties of these

samples in the composition range $\text{Mg}^{2+}/\text{Al}^{3+} = 0.25$ to 6.0 were similar, and a hydrotalcite-like layered double hydroxide material (LDH; JCPDS file 22-700) was observed in each case, giving a series of (00 l) peaks appearing as narrow symmetric lines at low angle, corresponding to the basal spacing and high order reflections. The purity of the phase, however, depended on the Mg/Al molar ratio. X-ray diffraction pattern of Mg/Al molar ratios of 0.25 and 0.5 showed the presence of AlOOH (boehmite) as a phase impurity with LDH as the major phase. Mg/Al molar ratios of 1.0 and 4.0 showed the X-ray pattern of single phase LDH compound which matched totally with the standard LDH pattern [15]. Generally, the sharpness and intensity of XRD were considered to be proportional to the crystallinity [16, 17]. Although the purely layered structure with characteristic and symmetric reflections could be obtained when Mg/Al molar ratio was equal to 1.0, the lower intensities and broader half-height widths at low 2θ angle were observed which indicated that the crystallinity of LDH Mg/Al 1.0 was poorer than that of the LDH Mg/Al 4.0. In the sample of LDH Mg/Al 6.0, the formation of MgCO_3 in addition to LDH was revealed. The appearance of MgCO_3 as an impurity was due to the increase of magnesium content. A closer examination of Fig. 1 revealed that the peak sharpness and intensity increased as the Mg/Al molar ratio was added from 0.25 to 4.0, indicating an improved crystallinity, and then decreased when the Mg/Al molar ratio was above 4.0. So, the sample LDH Mg/Al 4.0 possessed the highest crystallinity.

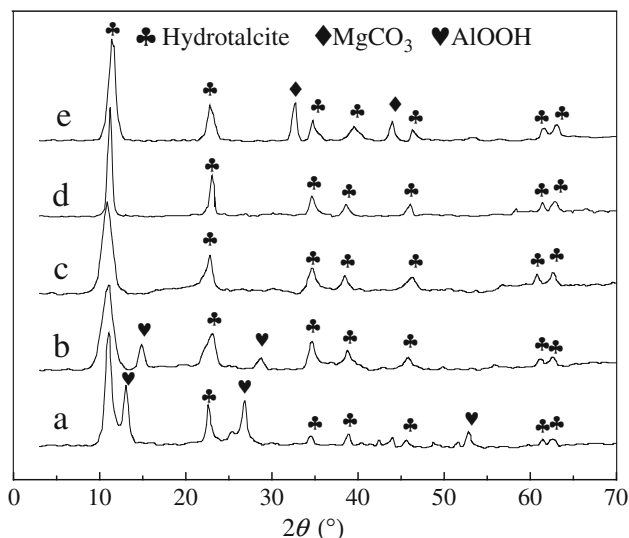


Fig. 1 X-ray diffraction patterns of the LDHs samples. *a* Mg/Al 0.25, *b* Mg/Al 0.5, *c* Mg/Al 1.0, *d* Mg/Al 4.0, *e* Mg/Al 6.0

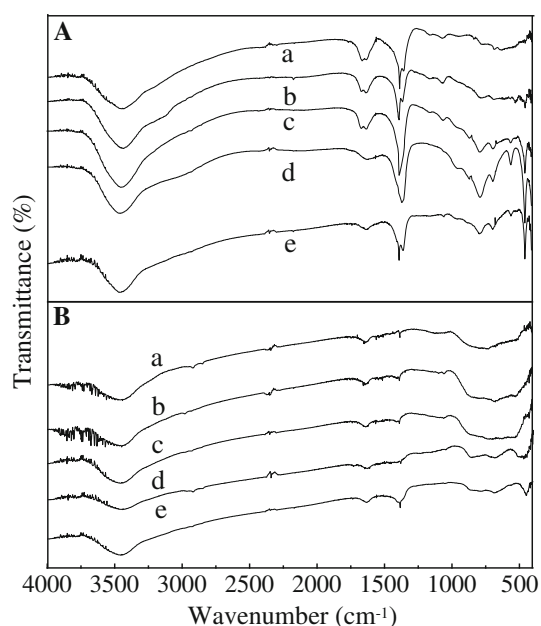


Fig. 2 FT-IR spectra of the LDHs and LDOs samples. **A** LDHs samples, **B** LDOs samples; *a* Mg/Al 0.25, *b* Mg/Al 0.5, *c* Mg/Al 1.0, *d* Mg/Al 4.0, *e* Mg/Al 6.0

3.1.2 FT-IR Spectra

The FT-IR spectra of the Mg–Al hydrotalcites with different Mg/Al molar ratios in the region 400–4000 cm^{-1} were shown in Fig. 2. For all the hydrotalcites with different Mg/Al molar ratios, the broad band was found at around 3450 cm^{-1} ($\nu_1\text{-OH}^{-1}$) and it was ascribable to the brucite-like layers (OH^{-} stretching vibration), caused by the interlayer water molecules and hydroxyl groups in the brucite-like layers [18]. In lower frequency region (Fig. 2A), a peak at about 1650 cm^{-1} ($\delta\text{-HOH}$) in all the LDHs samples could be attributed to the bending mode of interlayer water [18, 19]. However, a shoulder around 1650 cm^{-1} , or of a double band in the region 1640–1660 cm^{-1} , was observed in the cases of Mg/Al molar ratios of 0.25, 0.5 and 1.0 (≤ 1.0). This might indicate the presence of a very small amount of aluminum not incorporated in the hydrotalcite structure [19]. The carbonate anion in a symmetric environment was characterized by a D_{3h} planar symmetry, with three IR active absorption bands, as well as in the case of the free carbonate anion. In most hydrotalcites the three bands were observed at 1350–1380 cm^{-1} (ν_3), 850–880 cm^{-1} (ν_2) and 670–690 cm^{-1} (ν_4) [15]. This was almost what was observed for every hydrotalcite irrespective of the nature of the octahedral sheets suggesting full symmetry for the interlayer anions [20]. The three bands were observed only in the samples with Mg/Al molar ratios of 1.0 and 4.0, which implied the Mg/Al molar ratios of 1.0 and 4.0 had a rather symmetric structure for the interlayer anions. The main absorption

band of the carbonate anions was observed at 1370 cm^{-1} (ν_3) for all the LDHs samples. For the Mg/Al molar ratios of 0.25, 0.5 and 6.0, this peak split into a double band indicating a lowering of carbonate anion symmetry and the disordered nature of the interlayer, which caused the removal of the degeneracy of the ν_3 and ν_4 modes [15]. The appearance of some very faint absorption at 670–700 cm^{-1} for the Mg/Al molar ratios of 0.25 and 0.5 implying the disordered nature, and the band at 687 cm^{-1} for Mg/Al molar ratio of 4.0 was strongest in all other samples, showing that the above interpretation was justified. The lowering of the symmetry also caused the activation of the ν_1 mode around 1050 cm^{-1} , inactive when the carbonate anion retained its full symmetry [15, 19, 20]. The ν_1 vibrational mode of carbonate ions appeared at 1060 cm^{-1} . The above assumption was supported by the result that the ν_1 mode was found for the Mg/Al molar ratios of 0.25, 0.5, 1.0 and 6.0, but not for the Mg/Al molar ratios of 4.0. The results showed that the LDH Mg/Al 4.0 possessed high symmetry and ordered nature of the interlayer anions. The bands around 553 and 770 cm^{-1} could be assigned to translation modes of the hydroxyl groups mainly influenced by the trivalent aluminum but also influenced by probably Mg^{2+} in its coordination [19]. It could be seen that the band at 770 cm^{-1} were clearly observed for all the Mg/Al molar ratios, and the band at 553 cm^{-1} for the Mg/Al molar ratios of 1.0, 4.0 and 6.0, but not for 0.25 and 0.5. The intensity of the two bands was the highest for the Mg/Al molar ratios of 4.0. The appearance of absorption band at around 445 cm^{-1} ($\delta\text{ O-M-O}$) characteristic of lattice vibrations of [Mg, Al] octahedral sheets demonstrated the crystallization of the LDHs [21]. The intensity of the sharp peak at 445 cm^{-1} increased with decrease in Al concentration in the hydrotalcites with Mg/Al molar ratios of 0.25–4.0, and then decreased in the hydrotalcite with Mg/Al molar ratios of 6.0. The observed discrepancies among the LDHs with various Mg/Al molar ratios in FT-IR spectra were consistent with those in XRD patterns (Fig. 1). The samples with Mg/Al molar ratios of 1.0 and 4.0 showed pure the hydrotalcite pattern while the others showed impurities of AlOOH (Mg/Al 0.25 and 0.5) and MgCO_3 (Mg/Al 6.0).

The spectra of the calcined samples (LDOs) were different from those of the precursors (LDHs) (Fig. 2B). The ($\nu_1\text{-OH}^{-1}$) mode appeared around 3450 cm^{-1} , where the intensity of the band was obviously lower than that of the uncalcined samples (LDHs). The weak band at around 1640 cm^{-1} was observed, but the shoulder in the region disappeared for the LDO Mg/Al 0.25, 0.5 and 1.0 (≤ 1.0). The band appeared at around 1390 cm^{-1} (ν_3) which was about 20 cm^{-1} higher than that of the LDHs, and no splitting was found for all the LDO samples. The presence of a band of 678 cm^{-1} was only in the LDO Mg/Al 4.0 and

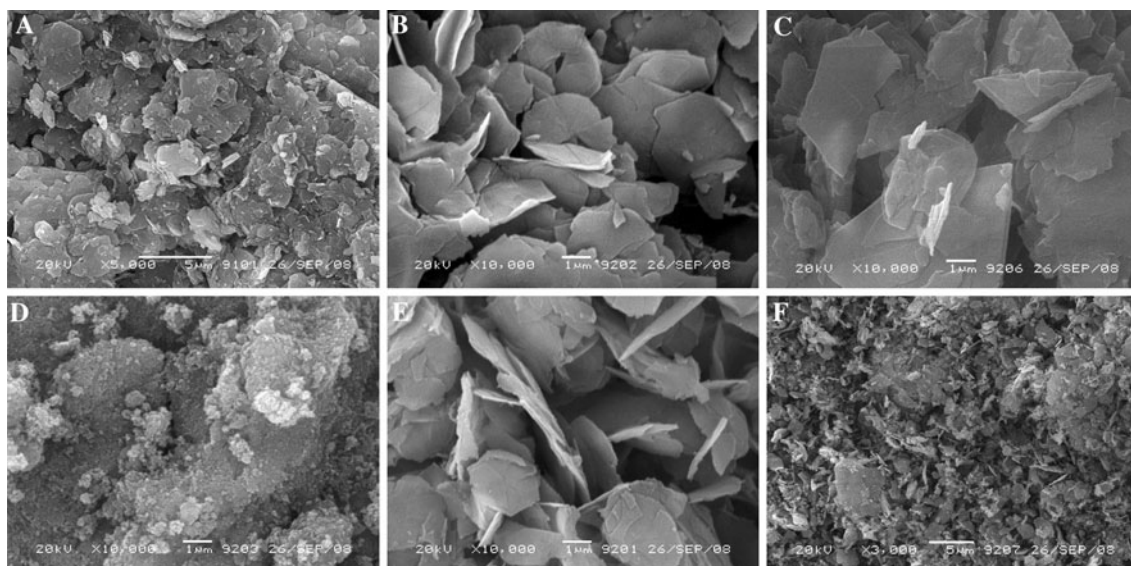


Fig. 3 SEM images of the LDHs and LDOs samples. **A** LDH Mg/Al 0.25, **B** LDH Mg/Al 4.0, **C** LDH Mg/Al 6.0, **D** LDO Mg/Al 0.25, **E** LDO Mg/Al 4.0, **F** LDO Mg/Al 6.0

6.0 samples. The peak at 452 cm^{-1} stood for the lattice vibrations of [Mg, Al] octahedral sheets, but also appeared only in the LDO Mg/Al 4.0 and 6.0 samples. There was a peak appearing at 864 cm^{-1} only in the LDO Mg/Al 4.0 sample, which implied the LDO Mg/Al 4.0 remained the hydroxalcite layered structure. Calcination at $500\text{ }^{\circ}\text{C}$ induced dehydration, dehydroxylation and decarbonation leading to the formation of mixed oxides of MgO and Al_2O_3 , and the FT-IR spectra of calcined samples reflected these changes [22].

3.1.3 SEM Images

In order to investigate the morphology for the LDHs and LDOs, the LDHs and LDOs with different Mg/Al molar ratios 0.25, 4.0 and 6.0 were observed with SEM (Fig. 3). Thin flat crystals indicating the layered structure were observed for all the LDH samples. The plate-plate overlapping of crystallites gave rise to interfaces that could accommodate extrinsic surface water, as well as other adsorbates. All the particles of the LDH Mg/Al 4.0 showed well-developed hexagonal plates with narrow size distribution ($2\text{--}4\text{ }\mu\text{m}$) and the samples could be seen to be made up of individual platelet particles in line with the typical morphology for hydroxalcite-like materials (Fig. 3B). This was in agreement with the XRD and FT-IR results mentioned above. The morphology and particle size of the calcined material LDO with Mg/Al 4.0 (Fig. 3E) was basically similar to those of the LDH precursor (Fig. 3B), where the hexagonally lamellar morphology was integrally preserved after calcination at $500\text{ }^{\circ}\text{C}$. It was interesting to note that the calcination process did not alter the

morphology and the size of the LDO Mg/Al 4.0 particles, similar to the result reported by Lei et al. [23]. This was in agreement with the assumption from IR that the LDO Mg/Al 4.0 remained the hydroxalcite layered structure (Fig. 2B). When the LDH sample with Mg/Al 0.25 was prepared, strong textural change was observed. The sample had irregular platelets forming aggregates only with little hexagonal plate-shaped particles (Fig. 3A). The calcination at $500\text{ }^{\circ}\text{C}$ made the layered structure of the LDO Mg/Al 0.25 disappear (Fig. 3D) and the inorganic layers were no more identified, which indicated calcination led to the destruction of the layered structure. For the sample LDH Mg/Al 6.0, individual platelets were still well observed with irregular and imperfect platelet crystals besides the perfect hexagonal platelets were observed (Fig. 3C). The typical hexagonal platelets were still identified after the calcination, and a lot of small particles and platelet aggregates appeared in the Fig. 3F, in accordance with the IR result for the LDO Mg/Al 6.0.

3.1.4 BET Surface Area

Table 2 showed the results of the BET for the LDHs and LDOs. The Mg/Al molar ratio in the samples had a strong influence on the surface areas. With increase in the Mg/Al molar ratio, the BET areas of the materials decreased from 172.92 to $53.14\text{ m}^2\text{ g}^{-1}$ for the LDHs samples, and from 237.92 to $92.03\text{ m}^2\text{ g}^{-1}$ for the LDOs samples. This increase in surface area after calcination correlated with the removal of water and CO_2 from the interlayer space and an increase in the pore volume. This behavior was similar to other hydroxalcite-like compounds and their homologous

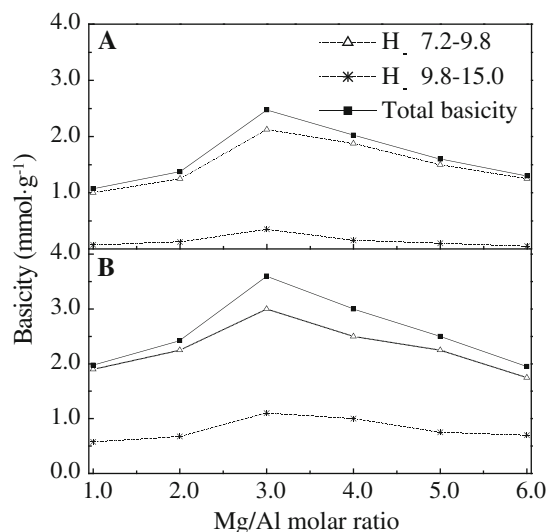
Table 2 BET surface area and base strength of Mg–Al hydrotalcites with different Mg/Al molar ratios

Sample	LDHs		LDOs	
	S_{BET} ($\text{m}^2 \text{g}^{-1}$)	Basic strength (H_-)	S_{BET} ($\text{m}^2 \text{g}^{-1}$)	Basic strength (H_-)
Mg/Al 0.25	172.92	–	237.92	–
Mg/Al 0.5	132.64	–	215.67	–
Mg/Al 1.0	111.12	$7.2 < H_- < 8.2$	201.24	$9.8 < H_- < 12.2$
Mg/Al 2.0	–	$8.2 < H_- < 9.8$	–	$12.2 < H_- < 15.0$
Mg/Al 3.0	98.72	$9.8 < H_- < 12.2$	189.23	$15.0 < H_- < 17.2$
Mg/Al 4.0	80.16	$9.8 < H_- < 12.2$	165.87	$15.0 < H_- < 17.2$
Mg/Al 5.0	–	$8.2 < H_- < 9.8$	–	$12.2 < H_- < 15.0$
Mg/Al 6.0	53.14	$7.2 < H_- < 8.2$	92.03	$9.8 < H_- < 12.2$

calcination products [16]. The calcination of hydrotalcite-like samples at 500 °C resulted in mesoporous mixed oxides with high surface areas. The LDO Mg/Al 0.25 had the highest surface area ($237.92 \text{ m}^2 \text{g}^{-1}$), while the LDO Mg/Al 6.0 had the lowest surface areas. This difference might be attributed to Al content in the Mg–Al hydrotalcite samples.

3.1.5 Surface Basicity

Though both basic and acidic sites are present in LDHs [23], it is reported that the synthesis of 1-methoxy-2-propanol should be closely related to the basic sites with moderate strength [4]. The basic strengths of various LDHs and LDOs were determined by using Hammett indicator and their basic strengths were in the ranges of 7.2–12.2 and 9.8–17.2, respectively (Table 2). The basicity of the Mg–Al hydrotalcites with different Mg/Al molar ratios was shown in Fig. 4. The main basic sites with H_- in the range of 7.2–9.8 (weak basic sites) and the other sites with H_- in the range of 9.8–15.0 (medium basic sites) were observed (Fig. 4), where all the samples had very few number of strong basic sites. The total basicity of the sample was increased gradually with the Mg/Al molar ratio and came up to the maximum value at the Mg/Al molar ratio of 3.0. However, with further increase in the Mg/Al molar ratio it was observed that the basicity was decreased. It was found that the maximum (2.5 mmol g^{-1} for the LDH and 3.6 mmol g^{-1} for the LDO) of the basic sites was at the Mg/Al molar ratio of 3.0. The similar results were reported by Xie et al. [24]. The basic strength and basicity of the LDHs samples were significantly lower than those of the LDOs. The total basicity in the ranges of 7.2–9.8 from the LDOs increased by 1.3–1.9 times compared with those from the LDHs. It was particularly noteworthy that the basicity in the ranges of 9.8–17.2 of the LDOs rose by about 3.1–7.7 times comparing with that of the LDHs, implying that the basicity in the ranges of 9.8–17.2 was significantly raised after calcination at 500 °C. There was

**Fig. 4** Basicity of Mg/Al hydrotalcites with different Mg/Al molar ratios. **A** LDHs, **B** LDOs

no marked difference in the basicity of the LDOs in the ranges of 9.8–17.2 (medium basic sites) between the LDO Mg/Al 3.0 and LDO Mg/Al 4.0 (Fig. 4B).

3.2 Catalytic Performance

The calcined hydrotalcites (LDOs) with different Mg/Al molar ratios were chosen for the catalytic test. The catalytic activity was tested in the synthesis of PM from methanol and PO (Fig. 5). The experimental results indicated that the catalytic activity (PO conversion and PM selectivity) was improved with increase in Mg content when the Mg/Al molar ratio was below 4.0, but when the Mg/Al molar ratio was above 4.0, the catalytic activity dropped. Clearly, such a tendency was basically correlated to that for the variation of the LDOs basicity in the ranges of 9.8–17.2 with various Mg/Al ratios (Fig. 4B). Another reason for the enhanced activity in the LDO Mg/Al 4.0 might be that the precursor LDH Mg/Al 4.0 showed better crystallinity in the XRD and

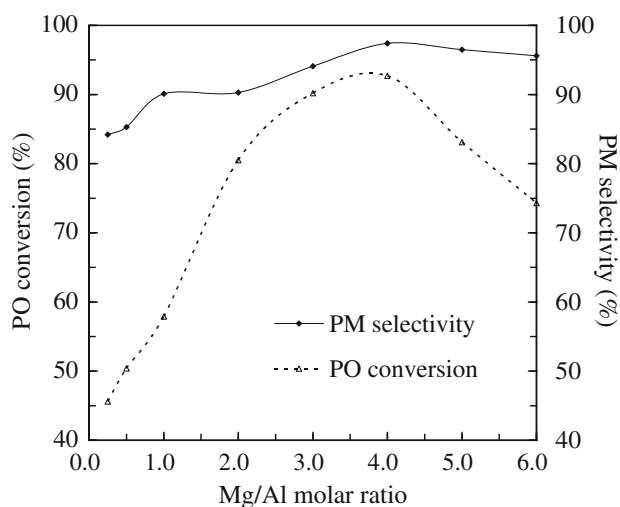


Fig. 5 Effect of Mg/Al molar ratio on the activity of the LDOs catalyst. Methanol/PO molar ratio 4.0, 1.0 wt% catalyst amount at 140 °C for 6 h

SEM data and the loss of the lamellar structure had previously been linked to poor activity [25]. The high crystallinity resulted in a regular arrangement of hydroxyl groups on the surface and a high density of appropriately acid–base balance [23]. The high catalytic activity and selectivity of the LDOs for the synthesis of PM were attributed to the presence of a high density of the medium basic sites. Calcination at high temperature decomposes the hydrotalcite into interactive, high surface area and well-dispersed mixed Mg–Al oxides which presents basic sites that are associated to structural hydroxyl groups as well as strong Lewis basic sites associated to $O^{2-}M^{n+}$ acid–base pairs [24]. The weak basic sites were associated with OH groups and the medium basic sites were assigned on M–O pairs [2, 4, 7]. The LDO Mg/Al 4.0 showed the highest PO conversion (92.7%) and PM selectivity (97.4%). The LDO Mg/Al 3.0 had the highest total basicity in all LDOs samples as well as similar basic strength (Table 2) and basicity in the ranges of 9.8–17.2 (medium basic sites) (Fig. 4B). However, the performance of the LDO Mg/Al 3.0 was lower than that of the Mg–Al LDO 4.0. This discrepancy might well be due to the reaction types and their influence on the reactivity of the acid–base sites playing a role in the mechanism. Under the conditions used in the present work, part of the medium basic sites of the LDO Mg/Al 3.0 likely did not take part in the reaction, but good correspondence existed between the number of the acid–base sites and the catalytic performance for the LDO Mg/Al 4.0. More appropriately acid–base balance on the surface of the Mg/Al 4.0 than Mg/Al 3.0 might result in a higher catalytic activity. So, the LDO Mg/Al 4.0 served as the catalyst for further researches on the optimization.

3.3 Orthogonal Experiment

Besides the pronounced effect of Mg/Al molar ratios on the catalytic activity of the catalyst, a number of factors such as temperature, reactant and catalyst concentrations, and reaction time could also affect the synthesis of PM since it was a liquid–solid two-phase reaction with a complicated reaction mechanism. The effects of temperature, methanol/PO molar ratio, catalyst amount and reaction time were studied. In this work, an orthogonal experimental design was conducted to investigate some pivotal reaction engineering parameters, which exerted strong influence on the PO conversion and PM selectivity.

As listed in Table 1, an orthogonal table of $L_{16}(4_4)$ was adopted to examine four variables as follows: temperature (T), methanol/PO molar ratio (M), catalyst amount (wt% of total reactants, A) and reaction time (t) at different levels. The observed PO conversion and PM selectivity varied remarkably with different parameters, suggesting that the optimization of reaction conditions for improving PO conversion and PM selectivity was a significant techno-economical necessity. The relative importance of factors to process indexes and the optimal set of factor levels were determined by margin and variance analysis according to the results shown in Table 3. In terms of the PO conversion from Table 4, the range of the factors was $T > M > t > A$, namely temperature ($R_{PO} = 158.8$) was the most important factor. The second important variable was the methanol/PO molar ratio ($R_{PO} = 108.2$), the third was reaction time

Table 3 Design and results of the orthogonal experiments

No.	T	M	A	t	PO conversion (%)	PM selectivity (%)
1	80	4:1	1.5	4	66.5	97.3
2	80	2:1	0.6	6	56.6	94.5
3	80	1:2	0.9	8	29.6	93.1
4	80	1:4	1.2	2	18.0	93.8
5	100	4:1	0.6	2	47.0	96.5
6	100	2:1	0.9	4	38.7	94.3
7	100	1:2	1.2	6	33.8	89.9
8	100	1:4	1.5	8	41.8	92.2
9	120	4:1	0.9	8	82.1	98.1
10	120	2:1	1.2	2	57.6	93.6
11	120	1:2	1.5	4	47.2	87.1
12	120	1:4	0.6	6	53.5	87.4
13	140	4:1	1.2	6	92.4	96.5
14	140	2:1	1.5	8	76.5	91.2
15	140	1:2	0.6	2	69.4	86.5
16	140	1:4	0.9	4	81.8	84.6

T temperature (°C), M methanol/PO molar ratio, A catalyst amount (wt%), t time (h)

Table 4 Margins of the conversion and PM selectivity, R_{PO} and R_{PM}

Factors	PO conversion (%)				R_{PO}	PM selectivity (%)				R_{PM}
	Sum of each level					Sum of each level				
	1	2	3	4		1	2	3	4	
T	170.7	161.3	240.4	320.1 ^a	158.8	378.7 ^a	372.9	366.2	358.8	19.9
M	288.1 ^a	229.4	179.9	195.0	108.2	388.4 ^a	373.6	356.6	358	31.8
A	226.5	232.2 ^a	201.8	231.9	30.4	364.9	370.1	373.8 ^a	367.8	8.9
t	192.0	234.1	236.3 ^a	230.0	44.3	370.4	363.3	368.3	374.6 ^a	11.3

T temperature (°C), M methanol/PO molar ratio, A catalyst amount (wt%), t time (h), R_{PO} range of PO conversion, R_{PM} range of PM selectivity

^a The optimum level

($R_{PO} = 44.3$). It was concluded that the optimal conditions were 140 °C, methanol/PO molar ratio 4.0, and catalyst amount 0.9 wt% for 6 h. As for the PM selectivity, the range of the factors was $M > T > t > A$, namely methanol/PO molar ratio ($R_{PM} = 31.8$) was the first effective factor, followed by temperature ($R_{PM} = 19.9$), and then reaction time ($R_{PM} = 11.3$), within the scope of selected reaction conditions. The optimum conditions were 80 °C, methanol/PO molar ratio 4.0, and catalyst amount 1.2 wt% for 8 h (Table 4).

The significance of each factor was further checked using analysis of variance (ANOVA) in Tables 5 and 6. For the PO conversion, temperature was highly significant (**), and methanol/PO molar ratio was significant (*), which corresponded with the margin analysis (Table 4). The variance analysis of the PM selectivity was different to that of the PO conversion, where methanol/PO molar ratio and temperature was highly significant (**). No obvious effect of reaction time and catalyst amount on the PO conversion and PM selectivity was observed (Table 4), as indicated by the low F value (Tables 5, 6). The most likely reason was that the reaction tended to equilibrium within the designed level of time.

In order to test the speculation on the time, the reaction time from 0.5 to 8 h was investigated in the conditions of 140 °C, catalyst amount 0.9 wt% and methanol/PO molar ratio 4.0. It was found that the PO conversion (0.5 h: 29.5%, 1.0 h: 80.3%, 2.0 h: 89.1%) significantly increased when reaction time was increased from 0.5 to 2 h, and then weakly increased when the time was more than 2 h (4.0 h: 92.8%, 6.0 h: 93.1%, 8.0 h: 94.1%). At the same time, PM selectivity (0.5 h: 97.5%, 1.0 h: 97.5%, 2.0 h: 97.4%) was stable when reaction time was increased from 0.5 to 2 h, and then slightly descended when the time was more than 2 h (4.0 h: 97.2%, 6.0 h: 97.0%, 8.0 h: 95.8%). The results confirmed our supposition on the effect of reaction time.

In view of production cost, the catalyst amount 0.9 wt% and reaction time 6 h were determined for further

experiments. The optimal conditions were predicted through the orthogonal experiment, but the optimal temperature and methanol/PO molar ratio were on the edge of the two levels in the orthogonal experiment. Hence, further studies in the extended range were conducted as follows, for the purpose of interpreting the reaction and improving operation of the process.

3.4 Influence of Temperature

The effect of the reaction temperature (from 80 to 160 °C) on the PO conversion and PM selectivity was studied (Fig. 6). Clearly, temperature strongly affected the PO conversion in the reaction. At moderate temperatures between 80 and 100 °C, the PO conversion was relatively low, which was possibly due to that PO might not be activated at a low reaction temperature. The PO conversion

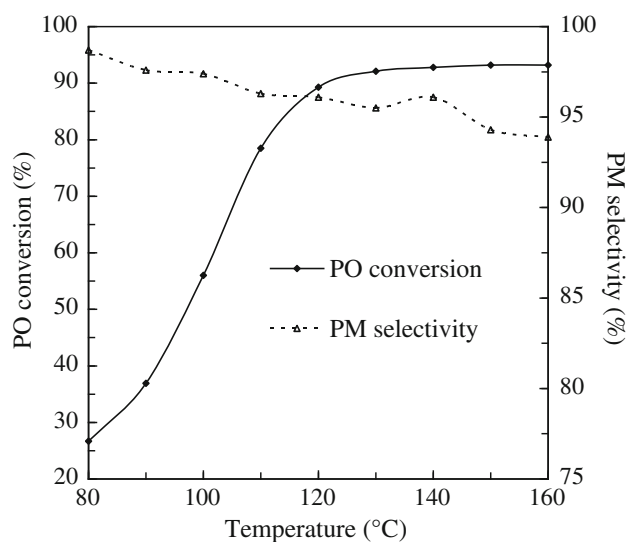


Fig. 6 Effect of reaction temperature on PO conversion and PM selectivity. Methanol/PO molar ratio 4.0, 0.9 wt% catalyst amount for 6 h

increased sharply with increase in temperature then reached a plateau value, where a nearly maximum PO conversion of 92.8% was obtained at 140 °C. Contrarily, the PM selectivity was decreased slowly with increase in temperature. When temperature was above 140 °C, the PM selectivity gradually declined because side reactions increased, implying that higher temperature were not favorable to the reaction. It had an optimal value, under which the effect of synergism was the best. As a result, 140 °C was selected as the feasible reaction temperature to achieve high PO conversion and PM selectivity.

3.5 Influence of Methanol/PO Molar Ratio

Based on the results above (Table 4, 5, 6), the reaction time (6 h) and catalyst amount (0.9 wt%) could be fixed, but the methanol/PO molar ratio needed to be tested further. In order to get the optimum factor, the six methanol/PO molar ratios, namely 3.0, 4.0, 5.0, 6.0, 7.0 and 8.0, were chosen and the experimental runs were conducted at 140 °C (Fig. 7). The optimum molar ratio was found to be 4.0. As represented in Fig. 7, by increasing methanol/PO molar ratio from 3.0 to 4.0, PO conversion and PM selectivity were smoothly increased. When the methanol/PO molar ratio was above 4.0, the PO conversion and PM selectivity had no significantly increase. Therefore, we could conclude that to elevate the PO conversion and PM selectivity, an excess methanol feed was effective to a certain extent. So, the optimum molar ratio was 4.0.

3.6 Reusability of the Catalyst

In order to evaluate the stability of the catalyst, reusability of the catalyst was studied under the optimal conditions. The catalyst was separated out by filtration under reduced pressure in the end of the reaction and then reused for the next run under the same conditions. The results as shown in Table 7 indicated that the PO conversion and PM selectivity was not affected even at the five runs with the reused catalyst. This finding implied that the catalyst could be recovered and recycled efficiently. Furthermore, the reusability of the catalyst would be further improved when the amount of the reactants and catalyst was increased, which needed to be further investigated.

4 Conclusions

The Mg/Al hydrotalcites were prepared by urea method. The effects of the Mg/Al molar ratio on the catalytic performance of the LDOs in the PM synthesis were studied. The LDO Mg/Al 4.0 catalyst revealed high activity for the synthesis of PM from PO and methanol. The catalyst showed the highest PO conversion of 93.2% and PM selectivity of 97.4%. An optimal balance of acid–base properties and high crystallinity made the LDO Mg/Al 4.0 an excellent catalyst in the synthesis reaction. As shown above, the activity might be further improved by optimizing reaction conditions. The reaction conditions for the

Table 5 Results of the ANOVA analysis from PO conversion

T temperature (°C), *M* methanol/PO molar ratio, *A* catalyst amount (wt%), *t* time (h), $F_{0.01}(3,12) = 5.95$ and $F_{0.05}(3,12) = 3.49$
* Significant, ** Highly significant

Source	Sum of squares of variance	Degree of freedom	Mean square	<i>F</i> value	<i>p</i>	Significance
T	4068.33	3	1356.11	10.44	>0.01	**
M	1718.98	3	572.99	4.41	>0.05	*
A	145.22	3	48.41	0.37		
t	361.36	3	120.45	0.93		
Error	389.55					
Total	6683.44					

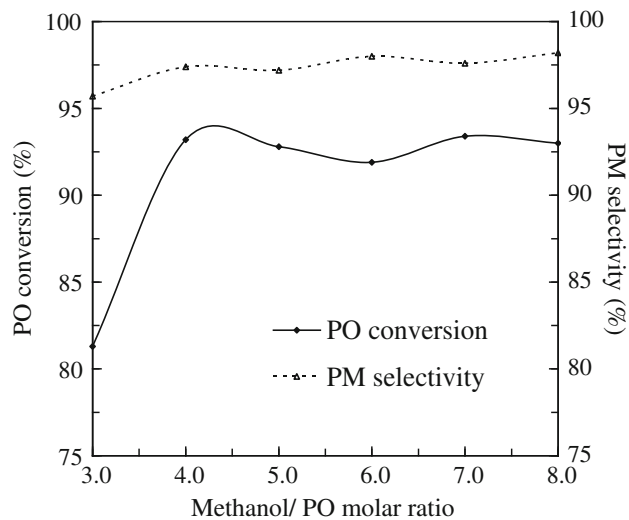
Table 6 Results of the ANOVA analysis from PM selectivity

T temperature (°C), *M* methanol/PO molar ratio, *A* catalyst amount (wt%), *t* time (h), $F_{0.01}(3,12) = 5.95$ and $F_{0.05}(3,12) = 3.49$
** Highly significant

Source	Sum of squares of variance	Degree of freedom	Mean square	<i>F</i> value	<i>p</i>	Significance
T	55.3	3	18.43	7.16	>0.01	**
M	168.075	3	56.025	21.76	>0.01	**
A	10.625	3	3.542	1.38		
t	16.575	3	5.59	2.15		
Error	7.725					
Total	258.3					

Table 7 The reusability of the LDO Mg/Al 4.0 catalyst

Used number	PO conversion (%)	PM selectivity (%)
1	93.3	97.4
2	93.2	97.8
3	92.5	97.4
4	92.7	97.2
5	91.9	97.0

**Fig. 7** Effect of methanol/PO molar ratio on PO conversion and PM selectivity

system were optimized to maximize the PO conversion (93.2%) and PM selectivity (97.4%) and almost all the PM in the reaction products was PPM. Optimum reaction conditions were obtained with methanol/PO molar ratio of 4.0, 0.9% catalyst (wt% of total reactants) at 140 °C for 6 h. The catalyst brought advantages such as high catalytic activity, easy separation by simple filtration, possible catalyst recycling and use of non-toxic and inexpensive catalyst. It is probable that the solid base catalyst becomes a practical alternative to soluble bases.

Acknowledgement This work was supported by Scientific Research Fund of Hunan Provincial Education Department of China through key-project (No. 08A080).

References

- Hootha MJ, Herberta RA, Hasemana JK, Orzecha DP, Johnsonb JD, Buchera JR (2004) *Toxicology* 204:123
- Cheng W, Wang W, Zhao Y, Liu L, Yang J, He M (2008) *Appl Clay Sci* 42:111
- Corley RA, Gies RA, Wu H, Weitz KK (2005) *Toxicol Lett* 156:193
- Zhang W, Wang H, Li Q, Dong Q, Zhao N, Wei W, Sun Y (2005) *Appl Catal A* 294:188
- Chitwood HC, Freure BT (1946) *J Am Chem Soc* 68:688
- Martins L, Hölderich W, Cardoso D (2008) *J Catal* 258:14
- Zhang W, Wang H, Wei W, Sun Y (2005) *J Mol Catal A* 231:83
- Fujita S-I, Bhanage BM, Aoki D, Ochiai Y, Iwasa N, Arai M (2006) *Appl Catal A* 313:151
- Atkins MP, Jones W, Chibwe M, US Patent 5,110,992 (1992)
- Malherbe F, Besse J-P, Wadel SR, Smith WJ (2000) *Catal Lett* 67:197
- Zeng HY, Deng X, Wang YJ, Liao KB (2009) *AIChE J* 55:1229
- Yang Z, Xie W (2007) *Fuel Processing Technol* 88:631
- Raj CBC, Quen HL (2005) *Chem Eng Sci* 60:5305
- JCPDS X-ray powder diffraction file, no. 22-700 (1986)
- Cavani F, Trifiro F, Vaccari A (1991) *Catal Today* 11:173
- Kannan S, Narayanan A, Swamy CS (1996) *J Mater Sci* 31:2353
- Costantino U, Marmottini F, Nocchetti M, Vivani R (1998) *Eur J Inorg Chem* 10:1439
- Dos Reis MJ, Silverio F, Tronto J, Valim JB (2004) *J Phys Chem Solids* 65:487
- Klopprogge TJ, Frost RL (1999) *J Solid State Chem* 146:506
- Hernandez-Moreno MJ, Ulibarri MA, Rendon JL, Serna CJ (1985) *Phys Chem Miner* 12:34
- Adachi-Pagano M, Forano C, Besse J-P (2003) *J Mater Chem* 13:1988
- Rao MM, Reddy BR, Jayalakshmi M, Jaya VS, Sridhar B (2005) *Mater Res Bull* 40:347
- Lei XD, Zhang FZ, Yang L, Guo XX, Tian YY, Fu SS, Li F, Evans DG, Duan X (2007) *AIChE J* 53:932
- Xie WL, Peng H, Chen LG (2006) *J Mol Catal A* 246:24
- Prinetto F, Tichit D, Teissier R, Coq B (2000) *Catal Today* 55:103